

1 Neurofeedback fMRI in the motor system elicits bi-directional changes in 2 activity and white-matter structure in the healthy adult human brain

3 **Authors:** Cassandra Sampaio-Baptista^{1,*}, Heather F. Neyedli^{1,2}, Zeena-Britt Sanders¹, Kata
4 Díosi¹, David Havard¹, YunYing Huang¹, Jesper L. R. Andersson¹, Michael Lührs³, Rainer
5 Goebel³ and Heidi Johansen-Berg¹

6

7 **Affiliations:**

8 1 Wellcome Centre for Integrative Neuroimaging, FMRIB, Nuffield Department of Clinical Neurosciences,
9 University of Oxford, John Radcliffe Hospital, Headington, Oxford OX3 9DU, UK

10 2 Department of Kinesiology, School of Health and Human Performance, Dalhousie University, 6230 South Street,
11 Halifax, Nova Scotia, B3H 4R2, Canada

12 3 Department of Cognitive Neuroscience, Maastricht University, Oxfordlaan 55, 6229, Maastricht, The Netherlands

13

14 **Correspondence should be addressed to:**

15 * Dr. Cassandra Sampaio-Baptista cassandra.sampaio.baptista@ndcn.ox.ac.uk

16

17 **Neurofeedback can be used to alter brain activity and is therefore an attractive tool for
18 neuromodulation in clinical contexts. Different contexts might call for different patterns of
19 activity modulation. For example, following stroke, alternative therapeutic strategies could
20 involve up or down-regulation of activity in the ipsilateral motor cortex. However, effects
21 of such strategies on activity and brain structure are unknown. In a proof of concept study
22 in healthy individuals, we showed that fMRI neurofeedback can be used to drive activity
23 up or down in ipsilateral motor cortex during hand movement. Given evidence for activity-
24 dependent white matter plasticity, we also tested effects of activity modulation on white
25 matter microstructure using diffusion tensor imaging (DTI). We show rapid opposing
26 changes in corpus callosum microstructure that depend on the direction of activity
27 modulation. Bidirectional modulation of ipsilateral motor cortex activity is therefore
28 possible, and results not only in online changes in activity patterns, but also in changes in
29 microstructure detectable 24 hours later.**

30

31 **Introduction**

32 Many neuropsychiatric and neurological conditions are associated with aberrant patterns of brain
33 activity so neuromodulation approaches that drive activity towards more favourable patterns are
34 of therapeutic interest. Neurofeedback (NF) taps into the brain's intrinsic capacity for activity
35 modulation and has been used in a variety of clinical conditions (Sitaram et al., 2017; Wang et
36 al., 2018). Functional magnetic resonance imaging (fMRI) NF provides a powerful approach for
37 spatially specific alteration in brain activity patterns and has been successfully used in humans
38 at rest (Shibata et al., 2011; Ramot et al., 2016), and during executed movements (Neyedli et al.,
39 2018) or cognitive tasks (Young et al., 2017), with studies showing encouraging behavioural or
40 physiological effects (Sitaram et al., 2017).

41 Following stroke, there are alterations in activity across the motor system, with changes in
42 activity in ipsilateral (contralesional) motor cortex a particular focus of interest (Johansen-Berg

43 et al., 2002a). Whether this activity should be suppressed or amplified is a matter of debate and
44 the optimal approach might well vary between patients, with suppression appropriate in less
45 impaired patients and amplification in more impaired patients. While there are several studies
46 testing bidirectional modulation of the motor system (in both healthy individuals and stroke
47 patients) using non-invasive brain stimulation (Nitsche and Paulus, 2000; Hesse et al., 2007;
48 Stagg et al., 2009; Lindenberg et al., 2010; Allman et al., 2016; Strube et al., 2016), the few NF
49 studies that targeted ipsilateral motor regions activity have thus far focused on suppressing it
50 only (Auer et al., 2015; Neyedli et al., 2017; Wang et al., 2018). Furthermore, the vast majority
51 of previous studies using NF in the motor system (whether in clinical or healthy populations)
52 have used motor imagery (deCharms et al., 2004; Chiew et al., 2012), but motor execution is
53 arguably more relevant to rehabilitation. Therefore, the current study aimed to address the degree
54 to which activity in ipsilateral motor cortex can be bidirectionally modified with fMRI NF in
55 healthy individuals during executed movements as a proof of concept test of how this approach
56 might be applied and tailored to the patient as an adjunct to neurorehabilitation.

57

58 Additionally, we explored the effects of NF-driven activity modulation on white matter
59 microstructure. In humans, studies using diffusion tensor imaging (DTI) have shown that both
60 long-term and short-term learning changes the structure of white matter pathways (Scholz et al.,
61 2009; Hofstetter et al., 2013). Most NF studies have focused on behavioural and functional brain
62 effects, and only two, including a EEG-NF study, have assessed NF effects on the structure of
63 long-range connections (Ghaziri et al., 2013; Marins et al., 2019). While DTI-derived measures
64 such as fractional anisotropy (FA) are nonspecific and modulated by a variety of white matter
65 features, changes in white matter with learning and experience have been related in part to
66 myelin increases in rodents (Sampaio-Baptista et al., 2013; Sampaio-Baptista et al., 2020).

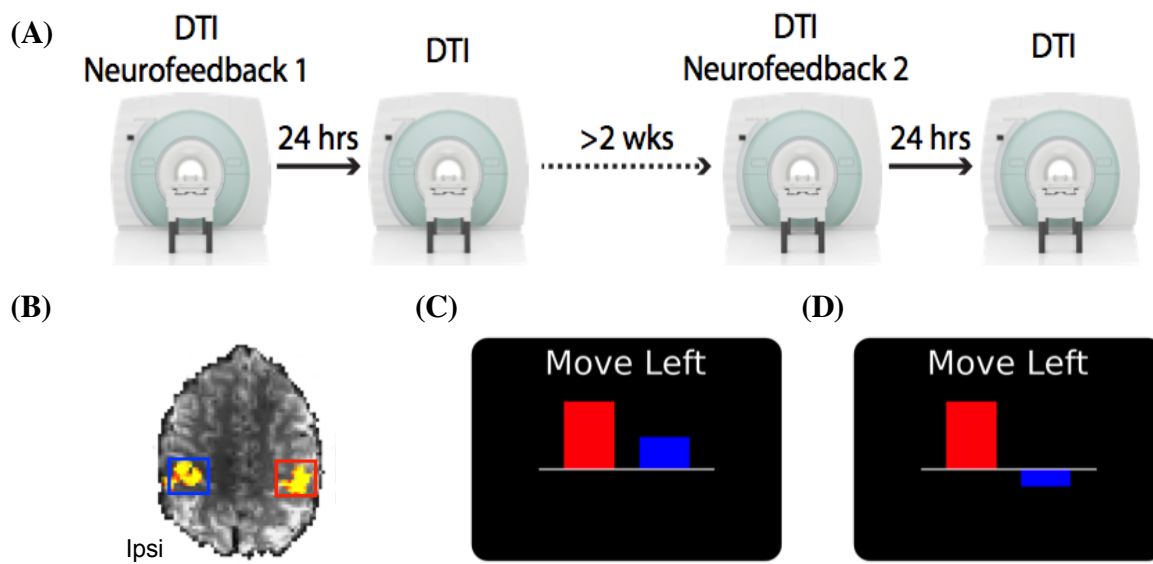
67 There is growing evidence that myelination can be bidirectionally altered by neuronal activity
68 (Demerens et al., 1996; Stevens et al., 1998) suggesting a bidirectionally-sensitive activity-
69 dependent mechanism might be the underlying driver of learning-related white matter changes
70 (Fields, 2005). Bidirectional NF modulation of focal activity, in combination with DTI measures
71 of white matter microstructure, provide a powerful approach to test these effects in humans. We
72 therefore employed real-time NF, using fMRI at 7 Tesla, to manipulate the activity of the
73 sensorimotor cortices (S1M1s) in opposite directions in two separate conditions, and tested for
74 effects on white matter structure against a sham group.

75

76 **Results**

77 Each participant was scanned 4 times and experienced two different NF conditions (only one NF
78 condition was experienced in each session), with DTI acquired before each condition and again
79 24 hours later (Fig. 1A). During NF, participants were instructed to modulate the height of two
80 bars (representing activity in ipsilateral and contralateral S1M1) on a visual display, by moving
81 *only* their left hand during 30s movement blocks, which alternated with 30s rest blocks. In the
82 ‘Association condition’ participants were required to co-activate both S1M1s (Fig. 1B, C), while
83 in the ‘Dissociation condition’ they were required to maximize contralateral S1M1 activity,
84 while minimizing ipsilateral S1M1 activity (Fig. 1B, D). Participants in the Sham group received
85 the same instructions but were shown the NF videos of a matched participant in the real NF
86 group, and experienced the same two conditions (Association and Dissociation). 80 scans were

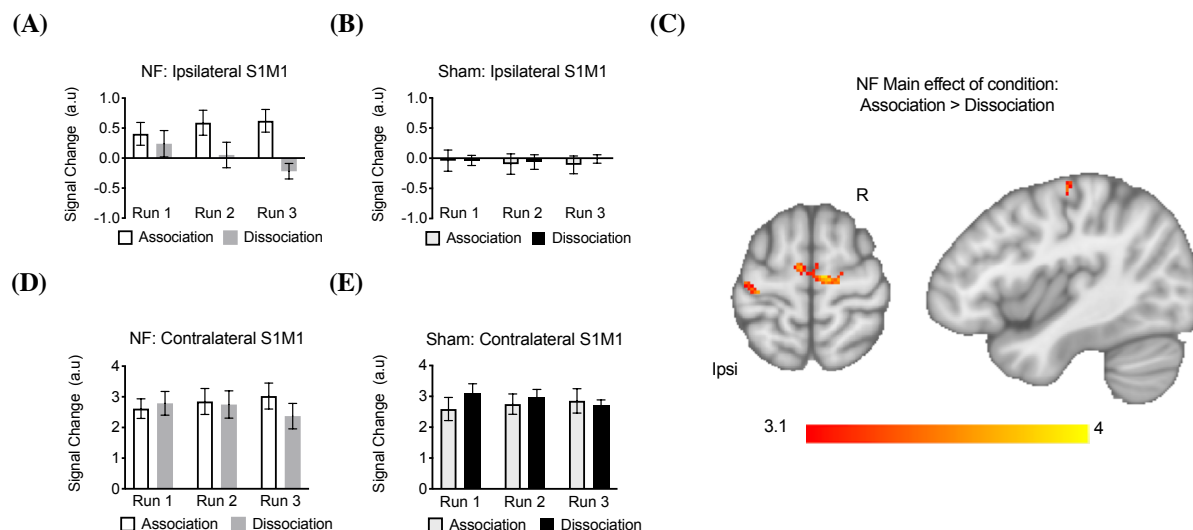
87 successfully completed, 28 participants were enrolled and complete data sets were obtained in 20
88 participants. For each feedback condition, participants trained for approximately 20 minutes (in 3
89 or 4 runs of ~6 minutes). EMG was used to monitor hand movements online and as expected the
90 muscle activity of the moving (left) hand was significantly higher than the non-moving (right)
91 hand and was similar between Real NF and Sham groups (Supplementary Fig. 1). A debriefing
92 questionnaire (Supplementary Table 1) revealed that both groups felt in control of the feedback
93 (Supplementary Table 2).



94
95 **Figure 1 Timeline and neurofeedback (NF) display.** (A) Participants in the real NF group and Sham
96 group experienced two different NF conditions, in a counterbalanced design, at least two weeks apart, with
97 DTI acquired before each NF session and again 24 hours later. (B) Functional localizer of an example
98 participant. S1M1 regions of interest were identified by asking the participants to move their right or left
99 fingers sequentially. Ipsi – Ipsilateral (C) Example NF display for the Association condition. (D) Example
100 NF display for the Dissociation condition.

101
102 We assessed fMRI activity to test whether participants could modulate S1M1 activity with
103 feedback as instructed. We first analysed signal change within the regions selected during NF
104 using a mixed ANOVA including within-subject factors of condition (Association, Dissociation)
105 and time (Run 1, 2, 3) and between-subject factor of group (Real, Sham). Instructions required
106 participants to increase ipsilateral S1M1 (iS1M1) activity for the Association condition and
107 decrease it for the Dissociation condition. Compared to the Sham group, participants in the NF
108 group were able to modulate activity in iS1M1 as instructed (Fig. 2A, B; main effect of
109 condition: $F_{(1,18)} = 8.53$, $p = 0.009$; condition x group interaction: $F_{(1,18)} = 12.082$, $p = 0.003$;
110 condition x time x group interaction $F_{(2,36)} = 5.03$, $p = 0.012$). Additionally, participants within
111 the NF group were able to modulate iS1M1 activity in opposite directions, with greater, and
112 increasing, activity in the Association condition compared to the Dissociation condition (Fig. 2A:
113 main effect of condition: $F_{(1,9)} = 32.045$, $p = 0.00031$; condition x time interaction: $F_{(2,18)} = 6.665$,
114 $p = 0.007$). By contrast, no effects of (or interactions with) group were found for the contralateral
115 S1M1 region of interest (ROI), with both groups strongly activating this ROI for both conditions

116 (Fig. 2D,E). Voxel-wise analysis within the NF group revealed specific clusters of significantly
117 greater activity in motor areas, including the ipsilateral hand knob, in the Association compared
118 to the Dissociation condition (Fig. 2C). No other significant clusters were found. The fMRI
119 results therefore demonstrate that the two NF conditions differ in iS1M1 activity, with greater
120 activity seen in the Association condition compared to the Dissociation condition. No significant
121 clusters were found in the sham group for the same comparison, showing that sham participants
122 did not differentially modulate their brain activity between conditions.

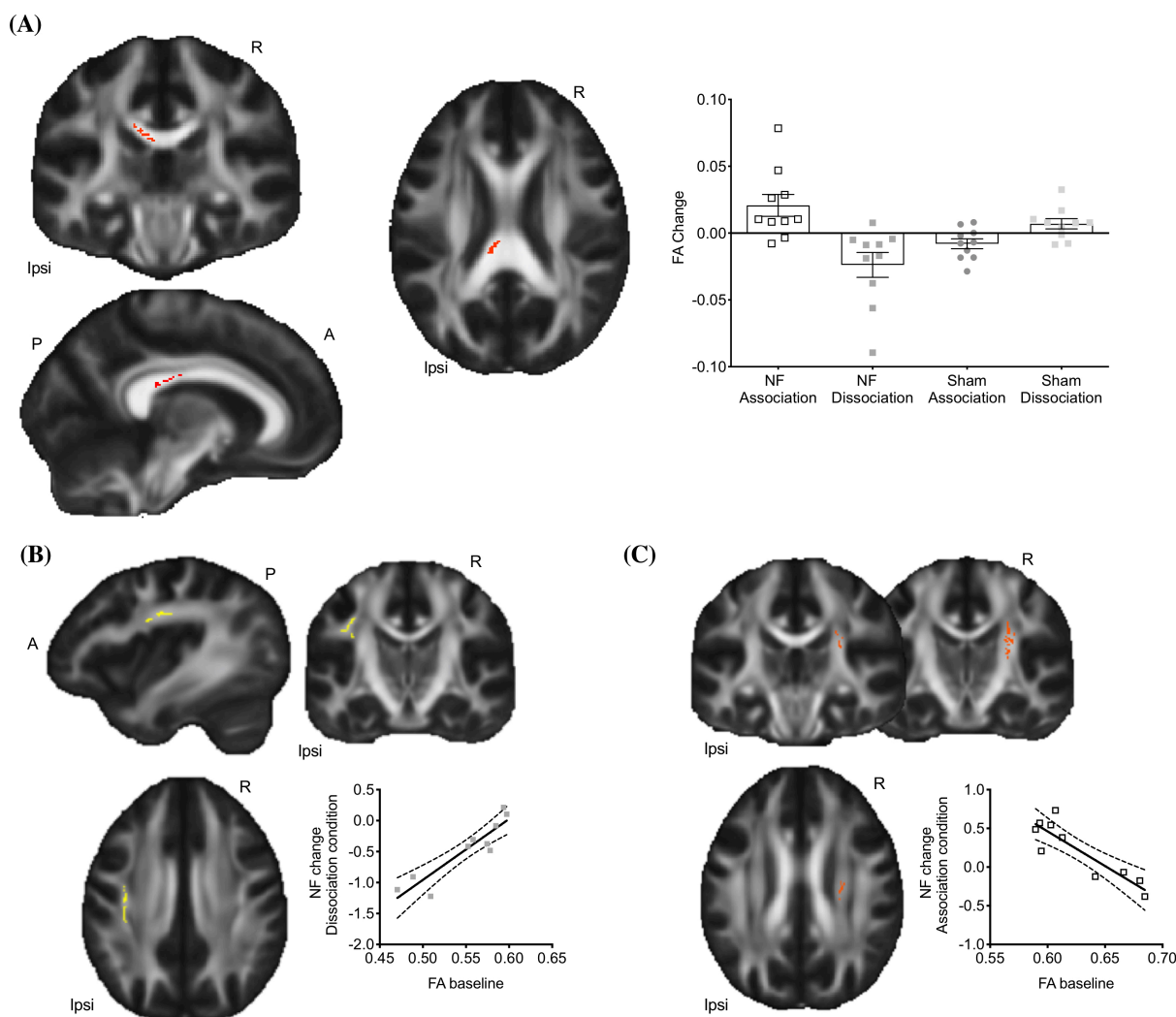


123
124 **Figure 2 Participants were able to modulate iS1M1 activity with feedback.** (A) Participants in the NF
125 group had lower iS1M1 activity in the Dissociation condition compared to the Association condition (B)
126 iS1M1 activity of the Sham group over the 3 runs (C) Voxel-wise analysis showing significantly higher
127 activity in the Association condition compared to the Dissociation condition in iS1M1 ($p < 0.05$,
128 corrected). (D-E) Instructions required participants to increase contralateral S1M1 (cS1M1) activity for
129 both conditions and both groups. Results showed no main effects or interactions with group, and no main
130 effects of time or condition on signal change within the cS1M1 ROI. There was a significant interaction
131 effect of condition x time which was further explored ($F_{(2,36)} = 6.25, p = 0.005$). This was driven by an
132 effect of time for the Dissociation condition ($F_{(2,36)} = 5.309, p = 0.01$), showing both groups decrease
133 activity over time within this condition. No effects of time were identified for the Association condition
134 ($F_{(2,36)} = 2.115, p = 0.135$). (D) Neurofeedback group contralateral activity in the S1M1 ROI over the 3
135 runs. (E) Sham group contralateral activity in the S1M1 ROI over the 3 runs. A.u. – Arbitrary units. Ipsi –
136 Ipsi-lateral Hemisphere, R - Right. Error bars represent SEM.

137
138 We went on to test whether this activity modulation resulted in alterations in white matter, as
139 measured by FA, an indirect measure of white matter microstructure previously shown to be
140 sensitive to learning-related white matter plasticity (Scholz et al., 2009; Sampaio-Baptista et al.,
141 2013). Voxel-wise FA maps were calculated from DTI scans acquired before and 24 hours after
142 each NF condition. To accommodate the mixed design nature of this study, FA change maps
143 (post-pre each condition) were first calculated for each condition and each group. Then maps of
144 the difference in FA change between conditions (Dissociation condition FA change –
145 Association condition FA change = condition difference) were calculated for each subject. The
146 resulting maps were then compared between groups.
147

148 We used a data-driven approach and performed whole-skeleton voxel-wise non-parametric
149 permutation testing of these between-group differences, which revealed a statistically significant
150 cluster in the corpus callosum, no other clusters were identified elsewhere in the brain (Fig. 3A)
151 ($p < 0.05$, corrected). This was driven by greater differences between conditions in FA change in
152 the NF group compared to the Sham group and reflected a positive FA change for the
153 Association condition and a negative FA change for the Dissociation condition within the NF
154 group (Fig. 3A). Tractography from this cluster identified pathways connecting sensorimotor and
155 parietal cortices (Supplementary Fig. 2).

156



157

158

Figure 3. NF training resulted in changes in white matter FA in the corpus callosum (A) Significant
159 FA cluster (in red) of the between-group contrast ($p = 0.05$, corrected). Plot on the right side represents
160 the individual participant mean FA change values within significant cluster represented in the FA map
161 and is shown for visualization of range of values and effect direction and not for inference. (B) Significant
162 positive correlation ($p < 0.05$, corrected) between baseline FA and NF fMRI change for the Dissociation
163 condition in the ipsilateral (left) superior longitudinal fasciculus (SLF) (represented in yellow). (C) A
164 trend (represented in red) towards a significant negative correlation ($p = 0.06$, corrected) between baseline
165 FA and NF change for the association condition was found in the contralateral (right) corticospinal tract.
166 Plots in (B) and (C) are shown for visualization of range of values and not for inference. Significant

167 cluster are superimposed on the FMRIB FA template. Ipsi – Ipsilateral Hemisphere, A-Anterior, P-
168 Posterior, R - Right. Error bars represent SEM.

169
170

171 We expected that changes in white matter structure would reflect successful modulation of
172 activity with neurofeedback. For each participant we therefore identified which of the two
173 neurofeedback conditions they performed best (see Supplementary Table 3 for more details). We
174 found a significant correlation between the fMRI activity change (run 3 – run 1) and change in
175 FA following this training session (Post24hrs – Baseline) ($r = 0.72$, $p = 0.02$, 2-tail). No such
176 correlation was found for the worse neurofeedback session ($r = -0.16$, $p = 0.66$, 2-tail). These
177 correlations were significantly different from each other (test of the difference between two
178 dependent correlations; $z = 2.058$, $p = 0.039$, 2-tail). This shows that, following effective
179 neurofeedback training, changes in structure are related to how effectively the participant
180 modulated iS1M1 activity.

181

182 Additionally, within the real NF group we tested whether baseline measures of FA correlated
183 with change in fMRI (run 3 – run 1) for each condition. Voxel-wise analysis of the whole
184 skeleton revealed a significant positive correlation ($p < 0.05$, corrected) between baseline FA and
185 NF fMRI change for the Dissociation condition in the ipsilateral (left) superior longitudinal
186 fasciculus (SLF) (Fig. 3B), suggesting that participants with higher baseline FA in this tract were
187 less able to use neurofeedback to reduce ipsilateral (left) sensorimotor activity as instructed. A
188 trend towards a significant negative correlation ($p = 0.06$, corrected) between baseline FA and
189 NF change was found in the contralateral (right) corticospinal tract for the Association condition
190 (Fig. 3C), suggesting that higher corticospinal FA at baseline is associated with lower
191 performance when instructed to increase ipsilateral activity with neurofeedback.

192
193

194 **Discussion**

195 Our results support the hypothesis that bidirectional activity modulation of ipsilateral
196 sensorimotor activity during executed hand movement can be achieved via neurofeedback and
197 that this results in rapid, directional, and anatomically specific changes in white matter structure.
198 This finding in healthy individuals is relevant to considering application of neurofeedback in
199 therapeutic contexts and in particular as an adjunct to motor neurorehabilitation after stroke.

200
201
202
203
204
205
206
207
208
209
210
211

201 The two conditions here could potentially be used as alternative interventions in stroke patients.
202 For instance, rebalancing of aberrant cortical activity by decreasing motor activity of the
203 ipsilateral (spared) hemisphere is a potential route for improving motor function after stroke
204 particularly in patients with low levels of impairment (Johansen-Berg et al., 2002b; Johansen-
205 Berg, 2003; Johansen-Berg, 2007), while enhancing activity in the ipsilateral motor cortex may
206 be beneficial for patients with more severe impairment (Bradnam et al., 2012; McDonnell and
207 Stinear, 2017). Future studies should assess these approaches in patients, where behavioural,
208 motor evoked-responses (MEPs) and MRI markers (Stinear et al., 2007) could be used as
209 predictors for tailoring the NF intervention to the individual, including which brain areas to
210 target and in which direction.

212 Activity in the ipsilesional S1M1 ROI showed clear modulation with NF, while activity in the
213 contralateral ROI remained fairly similar across NF and sham conditions, despite both real NF
214 conditions instructing increases in contralateral activity. Given that hand movements strongly
215 elicit contralateral sensorimotor activity in healthy participants it is likely that this is due to a
216 ceiling effect, with gains in activity not easily achieved. By contrast, there is typically very little
217 activity in ipsilateral S1M1 during this task in healthy individuals and so more scope for
218 modulation. Future studies employing several training sessions should assess whether further
219 training leads to progressive increases in contralateral activity, particularly in patient groups with
220 motor deficits or in older populations who may have lower activity in this region at baseline.

221

222 Our white matter results suggest that the focal activity modulation evoked by NF resulted in
223 changes in white matter microstructure that could be detected 24 hours later. Likely more than
224 one cellular mechanism underlies our structural findings. FA is modulated by several white
225 matter features such as myelination, axon density and caliber, and potentially by astrocyte
226 morphology, cell swelling, or changes in membrane fluidity (Sampaio-Baptista and Johansen-
227 Berg, 2017). Myelination is an attractive potential mechanism because neuronal activity can
228 bidirectionally regulate myelin formation and compaction and OPCs proliferation and
229 differentiation (Demerens et al., 1996; Stevens et al., 1998; Gibson et al., 2014) and such effects
230 occur over similar timescales to the ones used here (Xiao et al., 2016). For example, 30 minutes
231 of optogenetic stimulation of premotor neurons led to rapid increases in oligodendrocyte
232 precursor cells (OPCs) proliferation and differentiation within 24 hours (Gibson et al., 2014).
233 Furthermore, recently matured oligodendrocytes can form, extend and retract myelin segments
234 within 24 hours (Watkins et al., 2008; Czopka et al., 2013). Preexisting oligodendrocytes could
235 also contribute to myelin remodeling (Yeung et al., 2014; Dutta et al., 2018; Mitew et al., 2018),
236 however strong evidence for this process is currently scarce and the timescale at which this
237 occurs is unknown.

238

239 Importantly, new oligodendrocytes, formed during adulthood, play an essential role in new
240 motor skill acquisition (McKenzie et al., 2014), with impairments detected within a couple of
241 hours (Xiao et al., 2016), suggesting that learning is supported not only by neuronal changes,
242 such as synaptic plasticity, but also by adjunct changes in myelination (Long and Corfas, 2014).
243 Concurrently, other white matter structural properties such as axon density and caliber, astrocyte
244 morphology, cell swelling, or changes in membrane fluidity also occur in response to neuronal
245 activity and learning and could underlie some of the DTI effects (Blumenfeld-Katzir et al., 2011;
246 Sampaio-Baptista and Johansen-Berg, 2017; Sinclair et al., 2017).

247

248 The structural findings suggest that alterations in the elicited brain activity is a possible mediator
249 of previously described experience-related white matter changes in the human brain resulting
250 from behavioural interventions (Scholz et al., 2009; Hofstetter et al., 2013). However, given the
251 complex nature of the BOLD signal it is not straightforward to attribute BOLD fMRI increases
252 or decreases to either net excitation or net inhibition (Devor et al., 2007; Logothetis, 2008),
253 though some cellular specific mechanisms that contribute to BOLD have been recently described
254 (Uhlirova et al., 2016).

255

256 The anatomical site of the detected FA changes indicates that successful modulation of left
257 sensorimotor activity by performing left hand movements resulted in changes mainly in the
258 fibres that connect to the opposite hemisphere. This suggests that modulation of ipsilateral
259 activity occurred via callosal connections, resulting in structural alterations in the connections
260 between the two cortices. The corpus callosum is a relatively coherent fibre bundle as such small
261 changes might be easier to detect in this location, whereas white matter closer to the cortex
262 contains more crossing fibres and so effects of structural modulation on DTI metrics could be
263 harder to detect.

264

265 One challenge with clinical application of NF is that there is high variability in neurofeedback
266 success. Many studies identify ‘responders’ and ‘non-responders’ to NF and the individual
267 factors that determine NF success are not well understood. Here, we tested whether any baseline
268 variables correlated with neurofeedback success. We found that in the Dissociation condition,
269 higher ipsilateral SLF FA at baseline is associated with higher ipsilateral sensorimotor fMRI
270 change, while higher contralateral corticospinal FA at baseline is associated with lower
271 performance in increasing ipsilateral activity with neurofeedback. Both these results indicate that
272 high FA in motor-related pathways is associated with worse neurofeedback performance,
273 implying that highly structurally connected motor networks might be harder to modulate via
274 neurofeedback. These results open the possibility of using structural imaging to predict
275 neurofeedback performance, explain inter-individual variability and potentially tailor the
276 intervention to the needs of the participants. For instance, more neurofeedback sessions might be
277 necessary to change the activity of a highly structurally connected network.

278

279

280 Methods

281 Participants and design

282 All participants provided written informed consent in accordance with the University of Oxford
283 ethics committee approval of the protocol (MSD-IDREC-C1-2012-151).

284 28 right-handed participants (22-38 year old, 15 female) were recruited and scanned in a 7T
285 Siemens scanner 4 times (Fig. 1A).

286

287 Unbeknownst to the participants they were assigned to two different groups: Neurofeedback or
288 Sham. Total number of analyzed scans was 80 (NF group n=10x4=40; sham group n=10x4=40).
289 One participant in the NF group did not complete the experiment due to back pain and DTI was
290 not acquired in 1 participant due to scanner crashes. Four participants in the Sham group did not
291 complete the full study and data was not fully collected in further 2 Sham participants due to
292 scanner crashes.

293

294 Participants were blind to group assignment. The experimenter could not be blinded to group due
295 to limitations of the real time software. However, all participants received identical instructions
296 and experimental procedures were the same across the two groups with the exception of the
297 source of the feedback presented (see below). Each participant in each group was scanned under
298 two experimental conditions: association and Dissociation. For each condition participants were
299 scanned twice, 24 hours apart. The order of experimental conditions was counterbalanced across

300 participants and conditions were spaced at least 2 weeks apart (mean = 33.8 days, SD=16.3) (see
301 Fig. 1A).

302

303 **MRI data acquisition**

304 Imaging was performed on a 7.0T Siemens Magnetom MRI system (Siemens, Erlangen,
305 Germany) with a 32-channel head coil at the FMRIB Centre at the University of Oxford. For
306 each condition, scans were acquired over two days as follows:

307

308 *Day 1: fMRI Neurofeedback and DTI*

309 All fMRI data was acquired with a gradient echo planar image sequence (16 slices, 2 mm axial
310 plane, 2 x 2 mm² in plane resolution, repetition time (TR)=2000 ms; echo time (TE)=25 ms; flip
311 angle=90°). A whole brain echo planar image sequence was acquired for registration purposes
312 (60 slices, 2 mm axial plane, 2 x 2 mm² in plane resolution, TR=3500 ms; echo time=25 ms; flip
313 angle=90° field of view, 220 x 220mm).

314

315 *Functional localizer*

316 The functional localizer consisted of eight, 12-second tapping blocks, four blocks for each hand,
317 interspersed with 24 seconds rest. The participants saw the instructions 'Right Tap', 'Left Tap'
318 and 'Rest' displayed in white on a black background. Participants were told to use each finger in
319 sequence starting with their index finger and moving outward towards the little finger at a rate of
320 approximately 1 Hz, and to repeat the sequence until they saw the rest instruction. The results
321 from the real-time general linear model (GLM) of the localizer scan were used to select two
322 motor ROIs (18 x 18 x 10mm) for each participant, each centered over the peak of activation in
323 both hemispheres.

324

325 *DTI*

326 After the functional localizer we acquired whole brain diffusion-weighted volumes (64
327 directions; b-value = 1500 s/mm²; 80 slices; voxel size 1.5 x 1.5 x 1.5 mm³; TR=10 s; TE= 64
328 ms) including 5 volumes without diffusion weighting (b-value = 0 s/mm²), and also a separate
329 data set without diffusion weighting with opposite phase encoding for correction of susceptibility
330 induced distortions (b-value = 0 s/mm², 80 slices; voxel size 1.5 x 1.5 x 1.5 mm³; repetition time
331 (TR) = 10 s; echo time (TE) = 64 ms). The total acquisition time for DTI was about 10 minutes.

332

333 *Neurofeedback training*

334 Next, ~6 min feedback (FB) functional scans were acquired with a block design (30
335 seconds on, 30 seconds rest). In five sessions a fourth FB scan was acquired but only the first 3
336 training runs that were common to all participants were analysed.

337 Turbo-BrainVoyager software version 3.2 (Brain Innovation, Maastricht, The Netherlands;
338 Goebel, 2001) was used to calculate the BOLD signal in real time using a whole-brain voxel-
339 wise recursive GLM. The feedback signal was based on the averaged voxel time-course
340 extracted from the localized motor ROIs and the feedback image was updated each TR (2
341 seconds). Online motion correction in three dimensions, including translations and rotations were
342 used to correct for head movements during the scan.

343 A custom-made transmission control protocol (TCP) based network interface plug-in for Turbo-
344 Brain Voyager was used to transmit the preprocessed ROI time-course to Turbo-Feedback, a

345 custom-made software tool, which performed neurofeedback signal calculation and displayed the
346 resulting feedback to the participants.

347

348 Participants saw two vertical bars, representing the contralateral and ipsilateral hemispheric
349 activity, with a horizontal line delineating the center point. The equation used to calculate the
350 height of each bar was the following:

351 $\text{NF signal} = ([\text{ROI}_{\text{act}} - \text{ROI}_{\text{rest}}] / \text{ROI}_{\text{rest}})$

352 $\text{Bar Height on the display} = ([\text{ROI}_{\text{act}} - \text{ROI}_{\text{rest}}] / \text{ROI}_{\text{rest}}) / \text{MaxBarHeight}$

353 where ROI_{act} = current BOLD signal in ROI

354 ROI_{rest} = mean BOLD signal in the ROI during the previous rest blocks.

355 MaxBarHeight = maximum level of the bar

356

357 Positive values were represented above the centre point, and negative values below the centre
358 point (Fig 1C,D). The bar for contralateral (right hemisphere) activation was displayed on the left
359 as this hemisphere should be most active during left hand movement. The bar for ipsilateral (left
360 hemisphere) activation was displayed on the right.

361

362 *Sham Group*

363 Participants in the Sham group were matched to a participant in the NF group and received
364 feedback videos from that participant (rather than their feedback from their own brain activity).
365 This allowed the Sham participants to have a similar experience as the NF group. All scans and
366 instructions received by the Sham group were identical to those received by the NF group.

367

368 *Experimental conditions*

369 Two neurofeedback conditions were tested in separate sessions in both the NF and the Sham
370 group:

371 *Association condition* Participants were instructed to increase the size of both bars

372 *Dissociation condition* Participants were instructed to decrease the size of the bar on the right
373 side of the screen, while increasing the bar size on the left side

374 In this way, the goal of the Association condition was to maximise activation in both left and
375 right S1M1, whereas the goal of the Dissociation condition was to maximise right (contralateral)
376 S1M1 activity and minimize left (ipsilateral) S1M1 activity.

377

378 Participants were only told that the bars represented their brain activity. For both conditions
379 participants were asked to perform left hand movements in order to modulate the height of the
380 bars. The participants saw the instructions ‘Move Left’ or ‘Rest’ displayed in white on a black
381 background. Participants were allowed to use any left hand movement strategy to accomplish the
382 goal in each condition. Participants were instructed not to move their right hand during feedback
383 training and both arms were monitored on-line for movement using EMG. During the
384 instructions a list of example strategies were read but participants were told they could use any
385 other strategy as long as they did not move their right hand:

386 “*Open and close hand, move fingers, make grasping movements, move fingers sequentially or
387 randomly, imagine hand/finger movements, focus on moving hand or non-moving hand, increase
388 rate, force, size, of movement etc.*”

389

390 *Day 2: DTI*

391 24 hours after each NF training session DTI was again acquired with the same parameters as
392 above. For registration purposes, one structural image per subject was acquired during the
393 second session only using a T1 weighted, MPRAGE sequence with 1 x 1 x 1 mm³ isotropic
394 voxels (TR=2200 ms; TE=2.2 ms; flip angle 7°, field of view, 192x192; matrix=192x192).
395

396 **EMG Acquisition**

397 A Biopac system and AcqKnowledge software (Version 4.2) were used for EMG acquisition
398 during neurofeedback sessions. Due to technical difficulties we only acquired a full set of EMG
399 data in 7 participants in the NF group and 9 participants in the Sham group. We used two MRI
400 safe surface electrodes (ConMed corporation, USA) to record from the flexor carpi ulnaris
401 muscle and an additional electrode placed over the elbow olecranon was used as the ground
402 electrode. AcqKnowledge software was used to monitor and record muscle activity during the
403 feedback training acquisition with online MRI artifact and line noise correction.
404

405 **Neurofeedback questionnaire**

406 Following each feedback training session participants completed a questionnaire outside the
407 scanner (Supplementary Table 1). Participants reported on a scale of 1-5 how much control they
408 felt they had over the bar. Then a number of strategies for controlling the FB were presented and
409 participants were asked to report if they used the strategy and, if so, how successful they thought
410 the strategy was on a scale of 1-5.
411
412

413 **Data analysis**

414 **fMRI Preprocessing**

415 BOLD fMRI data for each subject were analyzed with FMRIB's expert analysis tool (FEAT,
416 version 5.98) from the FMRIB software library version 5.0 (www.fmrib.ox.ac.uk/fsl). Pre-
417 processing of the images included motion correction with FMRIB's Linear Image Registration
418 Tool (MCFLIRT), brain extraction with BET, spatial smoothing using a Gaussian kernel of 5
419 mm FWHM, and highpass temporal filtering of 150 s.

420 Functional data were first aligned to the whole brain scan and then to the subject's structural
421 image with linear registration (FMRIB's Linear Image Registration Tool, FLIRT), and then
422 optimized using Boundary-Based Registration (Greve and Fischl, 2009). For structural images
423 we used the anatomical processing script (fsl_anat) to robustly correct the bias-field and register
424 the images to standard MNI space. The resulting warp fields were then applied to the functional
425 images.

426 We used a voxel-based general linear model (GLM), as implemented in FEAT. For each
427 neurofeedback training scan, the block design paradigm (30 s hand movement plus feedback and
428 30 s rest) convolved with a gamma function, along with its temporal derivative, was used to
429 model the activation time course.
430

431 **ROI fMRI analysis of the Feedback Training**

432 After first-level Feat analysis, the tool featquery was used to extract the percentage signal change
433 of the defined motor ROIs. Mixed design ANOVA or Repeated-Measures ANOVA (SPSS
434 version 25) were used when appropriate to test for main effects of group, condition (Association,
435 Dissociation), NF run (1, 2, 3) and interaction effects between these variables. The significance
436 threshold used was p < 0.05.

437

438 **Group-level voxel-wise fMRI analysis**

439 To test for main effects of condition we used a within-subject fixed-effects second-level analysis
440 to calculate the average activation for the contrast of movement versus rest across the three
441 feedback scans per participant. The resulting maps were then fed into group level analysis using
442 FMRIB's Local Analysis of Mixed Effects (Woolrich et al., 2004).

443 We tested for differences between Association and Dissociation conditions with a paired t-test.
444 Z statistic images were thresholded using clusters determined by $Z > 3.1$ and a family-wise-
445 error-corrected cluster significance threshold of $p < 0.05$ was applied to the suprathreshold
446 clusters.

447

448

449 **DTI analysis**

450 DTI data were analysed with FMRIB's Diffusion Toolbox (FDT). Two sets of volumes without
451 diffusion-weighting were collected, with reversed phase-encode blips (i.e., one set with anterior-
452 posterior encoding and one with posterior-anterior), resulting in pairs of images with distortions
453 going in opposite directions. From these image pairs the susceptibility-induced off-resonance
454 field was estimated using a method similar to that described in (Andersson et al., 2003) as
455 implemented in FSL (Smith et al., 2004) All data were then corrected for susceptibility induced
456 distortions and for eddy current distortions and head movements with the FSL's eddy tool.

457 A diffusion tensor model was then fit to the data at each voxel using dtifit and voxel-wise maps
458 of fractional anisotropy (FA), mean diffusivity (MD), radial and axial diffusivity were estimated
459 for each subject and each timepoint. These maps were then analysed using Tract Based Spatial
460 Statistics (TBSS) (Smith et al., 2006). We performed unbiased registration by registering the
461 maps to the study specific template.

462 A mixed-design ANOVA is not accommodated by the general linear model (GLM) as
463 implemented in the FSL tool Randomise (<http://fsl.fmrib.ox.ac.uk/fsl/fslwiki/Randomise>). As such to be
464 able to test for group differences we have first computed the FA change (post-pre) maps for each
465 condition and each participant. We then calculated the difference between conditions for each
466 participant (Dissociation FA change – Association FA change = condition difference). These
467 maps were then compared between groups (NF vs Sham) with an unpaired t-test. This allows us
468 to test whether differences in FA change between conditions were greater in magnitude in the NF
469 group compared to the Sham group. Gender was used as a covariate (2/8 males/females in NF
470 group and 4/6 males/females in the Sham group).

471 We tested for group differences with an unpaired t-test by feeding these difference maps into
472 Randomise for permutation-based non-parametric testing of whole-skeleton FA. Clusters were
473 formed at $t > 1.7$ and tested for significance at $p < 0.05$, corrected for multiple comparisons
474 across space (Nichols and Holmes, 2002).

475

476 **Correlations between fMRI change and FA change**

477 We wished to test whether subjects who showed the most effective fMRI modulation with
478 feedback also had the greatest microstructural change in white matter. To do so, we first
479 calculated change in the fMRI activity (Run 3 – Run 1) for the iS1M1 ROI for each condition.
480 Rather than consider both conditions for each participant, we selected for each participant the
481 condition in which they performed best. By considering only one condition per participant we
482 could also ensure independence of data points for correlation calculation. Best performance was

483 defined as highest activity change in the instructed direction. 40% of the participants responded
484 best to the Association condition and 60% to the Dissociation condition, 50% of the participants
485 performed best in the first session regardless of condition (Supplementary Table 3). We tested
486 for correlations between this iS1M1 fMRI change and the corresponding FA change (Post24hrs-
487 Baseline) with Spearman's Rho ($p < 0.05$, 2-tail) (SPSS version 25).

488

489 **Tractography analysis**

490 We used tractography to identify the probabilistic connectivity map of the significant corpus
491 callosum FA cluster (i.e. cluster shown in Fig. 3A). First, for each participant, BEDPOSTX was
492 used to automatically determine the number of estimated fiber populations per brain voxel and to
493 fit estimates of principle diffusion direction for each population (Behrens et al., 2007). Then
494 PROBTRACKX (5000 samples, 0.5 mm step length, 2000 steps, 0.2 curvature threshold) was
495 used to follow these estimates in order to generate a probabilistic connectivity distribution, using
496 the FA cluster as a seed. The resulting individual participant probabilistic connectivity maps
497 were thresholded at 100. We then created two maps to illustrate the connectivity of the
498 significant FA cluster. To create the mean probability map the individual maps were then
499 overlapped across participants and the mean was extracted (Supplementary Fig. 2A). To
500 represent the tracts common to the population, the maps were binarized, added together and
501 colour-coded (Supplementary Fig. 2B).

502

503 **EMG analysis**

504 EMG data were band pass filtered offline from 20 Hz to 200 Hz, full-wave rectified and
505 converted to root mean square (RMS) using a 50 ms window period. For statistical comparison,
506 response-locked RMS-EMG activity was averaged from 0 to 30 s for each movement block, after
507 subtracting the 3 s before each movement onset as baseline. We used a Mixed Design ANOVA
508 (SPSS version 25) to test for effects of group, condition, run and hand.

509

510 **Questionnaire analysis**

511 A Wilcoxon signed-rank test was conducted to compare how much control the participants felt
512 they had over the feedback between conditions within group (Question A, Supplementary Table
513 1). A Mann-Whitney U test was used to compare how much control the participants felt they had
514 over the feedback between groups (Question A, Supplementary Table 1). A Mann-Whitney U
515 test was used to test if there were differences between groups in how successful the strategies
516 were perceived to be (Question B, Supplementary Table 1).

517

518

519 **Acknowledgments**

520 This work was supported by the Wellcome Trust (WT090955AIA and 110027/Z/15/Z to H J-B). The research was
521 further supported by Marie Curie Actions (Adaptive Brain Computations network PITN-GA-2008-290011) and by
522 the National Institute for Health Research (NIHR) Oxford Biomedical Research Centre based at Oxford University
523 Hospitals NHS Trust and University of Oxford. The views expressed are those of the author(s) and not necessarily
524 those of the NHS, the NIHR or the Department of Health. The Wellcome Centre for Integrative Neuroimaging is
525 supported by core funding from the Wellcome Trust (203139/Z/16/Z). The authors would like to thank N. Filippini,
526 S. Foxley and the radiography team for operating the 7T scanner, T. Makin and F. Eippert for assistance with the
527 EMG, S. Sotiropoulos for assistance with the 3D tractography pictures, and W. Richardson, T. Makin and J. O'Shea
528 for the useful comments on the manuscript.

529

530

531 **Author contribution**

532 C.S-B. designed the study, collected and analysed the data. H.N. collected data and provided assistance with data
533 analysis. Z.B.S. collected and analysed data. D.H and K. D. collected data. Y.H. provided assistance with EMG data
534 analysis. J.A., M.L. and R.G. developed and provided assistance with data collection methods and analysis. H.J-B
535 designed the study and supervised the project. C.S-B wrote the manuscript and all authors edited it.

537 **References**

538 Allman C, Amadi U, Winkler AM, Wilkins L, Filippini N, Kischka U, Stagg CJ, Johansen-Berg H (2016)
539 Ipsilesional anodal tDCS enhances the functional benefits of rehabilitation in patients after stroke. *Sci
540 Transl Med* 8:330re331.

541 Andersson JL, Skare S, Ashburner J (2003) How to correct susceptibility distortions in spin-echo echo-planar
542 images: application to diffusion tensor imaging. *Neuroimage* 20:870-888.

543 Auer T, Schweizer R, Frahm J (2015) Training Efficiency and Transfer Success in an Extended Real-Time
544 Functional MRI Neurofeedback Training of the Somatomotor Cortex of Healthy Subjects. *Front Hum
545 Neurosci* 9:547.

546 Behrens TEJ, Berg HJ, Jbabdi S, Rushworth MFS, Woolrich MW (2007) Probabilistic diffusion tractography with
547 multiple fibre orientations: What can we gain? *Neuroimage* 34:144-155.

548 Blumenfeld-Katzir T, Pasternak O, Dagan M, Assaf Y (2011) Diffusion MRI of structural brain plasticity induced
549 by a learning and memory task. *PLoS One* 6:e20678.

550 Bradnam LV, Stinear CM, Barber PA, Byblow WD (2012) Contralesional hemisphere control of the proximal
551 paretic upper limb following stroke. *Cereb Cortex* 22:2662-2671.

552 Chiew M, LaConte SM, Graham SJ (2012) Investigation of fMRI neurofeedback of differential primary motor
553 cortex activity using kinesthetic motor imagery. *Neuroimage* 61:21-31.

554 Czopka T, Ffrench-Constant C, Lyons DA (2013) Individual oligodendrocytes have only a few hours in which to
555 generate new myelin sheaths in vivo. *Dev Cell* 25:599-609.

556 deCharms RC, Christoff K, Glover GH, Pauly JM, Whitfield S, Gabrieli JD (2004) Learned regulation of spatially
557 localized brain activation using real-time fMRI. *Neuroimage* 21:436-443.

558 Demerens C, Stankoff B, Logak M, Anglade P, Allinquant B, Couraud F, Zalc B, Lubetzki C (1996) Induction of
559 myelination in the central nervous system by electrical activity. *Proc Natl Acad Sci U S A* 93:9887-9892.

560 Devor A, Tian P, Nishimura N, Teng IC, Hillman EM, Narayanan SN, Ulbert I, Boas DA, Kleinfeld D, Dale AM
561 (2007) Suppressed neuronal activity and concurrent arteriolar vasoconstriction may explain negative blood
562 oxygenation level-dependent signal. *J Neurosci* 27:4452-4459.

563 Dutta DJ, Woo DH, Lee PR, Pajevic S, Bukalo O, Huffman WC, Wake H, Basser PJ, SheikhBahaei S, Lazarevic V,
564 Smith JC, Fields RD (2018) Regulation of myelin structure and conduction velocity by perinodal
565 astrocytes. *Proc Natl Acad Sci U S A* 115:11832-11837.

566 Fields RD (2005) Myelination: an overlooked mechanism of synaptic plasticity? *Neuroscientist* 11:528-531.

567 Ghaziri J, Tucholka A, Larue V, Blanchette-Sylvestre M, Reyburn G, Gilbert G, Levesque J, Beauregard M (2013)
568 Neurofeedback training induces changes in white and gray matter. *Clin EEG Neurosci* 44:265-272.

569 Gibson EM, Purger D, Mount CW, Goldstein AK, Lin GL, Wood LS, Inema I, Miller SE, Bieri G, Zuchero JB,
570 Barres BA, Woo PJ, Vogel H, Monje M (2014) Neuronal activity promotes oligodendrogenesis and
571 adaptive myelination in the mammalian brain. *Science* 344:1252304.

572 Greve DN, Fischl B (2009) Accurate and robust brain image alignment using boundary-based registration.
573 *Neuroimage* 48:63-72.

574 Hesse S, Werner C, Schonhardt EM, Bardeleben A, Jenrich W, Kirker SG (2007) Combined transcranial direct
575 current stimulation and robot-assisted arm training in subacute stroke patients: a pilot study. *Restor Neurol
576 Neurosci* 25:9-15.

577 Hofstetter S, Tavor I, Tzur Moryosef S, Assaf Y (2013) Short-term learning induces white matter plasticity in the
578 fornix. *J Neurosci* 33:12844-12850.

579 Johansen-Berg H (2003) Motor physiology: a brain of two halves. *Current Biology* 13:R802-R804.

580 Johansen-Berg H (2007) Functional imaging of stroke recovery: what have we learnt and where do we go from
581 here? *Int J Stroke* 2:7-16.

582 Johansen-Berg H, Rushworth MF, Bogdanovic MD, Kischka U, Wimalaratna S, Matthews PM (2002a) The role of
583 ipsilateral premotor cortex in hand movement after stroke. *Proc Natl Acad Sci U S A* 99:14518-14523.

584 Johansen-Berg H, Dawes H, Guy C, Smith S, Wade D, Matthews P (2002b) Correlation between motor
585 improvements and altered fMRI activity after rehabilitative therapy. *Brain* 125:2731.
586 Lindenberg R, Renga V, Zhu LL, Nair D, Schlaug G (2010) Bihemispheric brain stimulation facilitates motor
587 recovery in chronic stroke patients. *Neurology* 75:2176-2184.
588 Logothetis NK (2008) What we can do and what we cannot do with fMRI. *Nature* 453:869-878.
589 Long P, Corfas G (2014) Neuroscience. To learn is to myelinate. *Science* 346:298-299.
590 Marins T, Rodrigues EC, Bortolini T, Melo B, Moll J, Tovar-Moll F (2019) Structural and functional connectivity
591 changes in response to short-term neurofeedback training with motor imagery. *Neuroimage* 194:283-290.
592 McDonnell MN, Stinear CM (2017) TMS measures of motor cortex function after stroke: A meta-analysis. *Brain*
593 Stimul 10:721-734.
594 McKenzie IA, Ohayon D, Li H, de Faria JP, Emery B, Tohyama K, Richardson WD (2014) Motor skill learning
595 requires active central myelination. *Science* 346:318-322.
596 Mitew S, Gobius I, Fenlon LR, McDougall SJ, Hawkes D, Xing YL, Bujalka H, Gundlach AL, Richards LJ,
597 Kilpatrick TJ, Merson TD, Emery B (2018) Pharmacogenetic stimulation of neuronal activity increases
598 myelination in an axon-specific manner. *Nat Commun* 9:306.
599 Neyedli HF, Sampaio-Baptista C, Kirkman MA, Havard D, Luhrs M, Ramsden K, Flitney DD, Clare S, Goebel R,
600 Johansen-Berg H (2017) Increasing lateralized motor activity in younger and older adults using Real-time
601 fMRI during executed movements. *Neuroscience*.
602 Neyedli HF, Sampaio-Baptista C, Kirkman MA, Havard D, Luhrs M, Ramsden K, Flitney DD, Clare S, Goebel R,
603 Johansen-Berg H (2018) Increasing Lateralized Motor Activity in Younger and Older Adults using Real-
604 time fMRI during Executed Movements. *Neuroscience* 378:165-174.
605 Nichols TE, Holmes AP (2002) Nonparametric permutation tests for functional neuroimaging: a primer with
606 examples. *Hum Brain Mapp* 15:1-25.
607 Nitsche MA, Paulus W (2000) Excitability changes induced in the human motor cortex by weak transcranial direct
608 current stimulation. *J Physiol* 527 Pt 3:633-639.
609 Ramot M, Grossman S, Friedman D, Malach R (2016) Covert neurofeedback without awareness shapes cortical
610 network spontaneous connectivity. *Proc Natl Acad Sci U S A* 113:E2413-2420.
611 Sampaio-Baptista C, Johansen-Berg H (2017) White Matter Plasticity in the Adult Brain. *Neuron* 96:1239-1251.
612 Sampaio-Baptista C, Valles A, Khrapitchev AA, Akkermans G, Winkler AM, Foxley S, Sibson NR, Roberts M,
613 Miller K, Diamond ME, Martens GJM, De Weerd P, Johansen-Berg H (2020) White matter structure and
614 myelin-related gene expression alterations with experience in adult rats. *Prog Neurobiol*:101770.
615 Sampaio-Baptista C, Khrapitchev AA, Foxley S, Schlagheck T, Scholz J, Jbabdi S, DeLuca GC, Miller KL, Taylor
616 A, Thomas N, Kleim J, Sibson NR, Bannerman D, Johansen-Berg H (2013) Motor skill learning induces
617 changes in white matter microstructure and myelination. *J Neurosci* 33:19499-19503.
618 Scholz J, Klein MC, Behrens TE, Johansen-Berg H (2009) Training induces changes in white-matter architecture.
619 *Nat Neurosci* 12:1370-1371.
620 Shibata K, Watanabe T, Sasaki Y, Kawato M (2011) Perceptual learning incepted by decoded fMRI neurofeedback
621 without stimulus presentation. *Science* 334:1413-1415.
622 Sinclair JL, Fischl MJ, Alexandrova O, Hebeta M, Grothe B, Leibold C, Kopp-Scheinplug C (2017) Sound-Evoked
623 Activity Influences Myelination of Brainstem Axons in the Trapezoid Body. *J Neurosci* 37:8239-8255.
624 Sitaram R, Ros T, Stoeckel L, Haller S, Scharnowski F, Lewis-Peacock J, Weiskopf N, Blefari ML, Rana M, Oblak
625 E, Birbaumer N, Sulzer J (2017) Closed-loop brain training: the science of neurofeedback. *Nat Rev
626 Neurosci* 18:86-100.
627 Smith SM, Jenkinson M, Johansen-Berg H, Rueckert D, Nichols TE, Mackay CE, Watkins KE, Ciccarelli O, Cader
628 MZ, Matthews PM, Behrens TE (2006) Tract-based spatial statistics: voxelwise analysis of multi-subject
629 diffusion data. *Neuroimage* 31:1487-1505.
630 Smith SM, Jenkinson M, Woolrich MW, Beckmann CF, Behrens TE, Johansen-Berg H, Bannister PR, De Luca M,
631 Drobniak I, Flitney DE, Niazy RK, Saunders J, Vickers J, Zhang Y, De Stefano N, Brady JM, Matthews
632 PM (2004) Advances in functional and structural MR image analysis and implementation as FSL.
633 *Neuroimage* 23 Suppl 1:S208-219.
634 Stagg CJ, Best JG, Stephenson MC, O'Shea J, Wylezinska M, Kincses ZT, Morris PG, Matthews PM, Johansen-
635 Berg H (2009) Polarity-sensitive modulation of cortical neurotransmitters by transcranial stimulation. *J
636 Neurosci* 29:5202-5206.
637 Stevens B, Tanner S, Fields RD (1998) Control of myelination by specific patterns of neural impulses. *J Neurosci*
638 18:9303-9311.

639 Stinear CM, Barber PA, Smale PR, Coxon JP, Fleming MK, Byblow WD (2007) Functional potential in chronic
640 stroke patients depends on corticospinal tract integrity. *Brain* 130:170-180.
641 Strube W, Bunse T, Nitsche MA, Nikolaeva A, Palm U, Padberg F, Falkai P, Hasan A (2016) Bidirectional
642 variability in motor cortex excitability modulation following 1 mA transcranial direct current stimulation in
643 healthy participants. *Physiol Rep* 4.
644 Uhlirova H et al. (2016) Cell type specificity of neurovascular coupling in cerebral cortex. *Elife* 5.
645 Wang T, Mantini D, Gillebert CR (2018) The potential of real-time fMRI neurofeedback for stroke rehabilitation: A
646 systematic review. *Cortex* 107:148-165.
647 Watkins TA, Emery B, Mulinyawe S, Barres BA (2008) Distinct stages of myelination regulated by gamma-
648 secretase and astrocytes in a rapidly myelinating CNS coculture system. *Neuron* 60:555-569.
649 Woolrich MW, Behrens TE, Beckmann CF, Jenkinson M, Smith SM (2004) Multilevel linear modelling for fMRI
650 group analysis using Bayesian inference. *Neuroimage* 21:1732-1747.
651 Xiao L, Ohayon D, McKenzie IA, Sinclair-Wilson A, Wright JL, Fudge AD, Emery B, Li H, Richardson WD
652 (2016) Rapid production of new oligodendrocytes is required in the earliest stages of motor-skill learning.
653 *Nat Neurosci* 19:1210-1217.
654 Yeung MS, Zdunek S, Bergmann O, Bernard S, Salehpour M, Alkass K, Perl S, Tisdale J, Possnert G, Brundin L,
655 Druid H, Frisen J (2014) Dynamics of oligodendrocyte generation and myelination in the human brain. *Cell*
656 159:766-774.
657 Young KD, Siegle GJ, Zotev V, Phillips R, Misaki M, Yuan H, Drevets WC, Bodurka J (2017) Randomized
658 Clinical Trial of Real-Time fMRI Amygdala Neurofeedback for Major Depressive Disorder: Effects on
659 Symptoms and Autobiographical Memory Recall. *Am J Psychiatry* 174:748-755.
660